International Journal of Precision Engineering and Manufacturing (2022) 23:1133–1141
https://doi.org/10.1007/s12541-022-00666-7

Online ISSN 2005-4602
Print ISSN 2234-7593

REGULAR PAPER

Use of a Virtual Polyhedron for Interim Checking of the Volumetric and Geometric Errors of Machine Tools

Kwang-Il Lee[1] · Heung-Ki Jeon[2] · Jae-Chang Lee[3] · Seung-Han Yang[2]

Received: 6 October 2021 / Revised: 28 February 2022 / Accepted: 20 April 2022 / Published online: 22 August 2022

Abstract

Volumetric and geometric errors should be periodically checked to ensure that the accuracy of machine tools remains within the tolerable range. However, existing methods require complex devices, and are thus unsuitable for cost-effective interim error checks. We present a simple, rapid and cost-effective method for interim error checks. The measurement paths are constructed using a virtual polyhedron; volumetric errors are checked by calculating the coordinates of the vertices using the measured side lengths. The tool is sequentially moved to each vertex, and the side lengths are measured using a double ball-bar. As the virtual polyhedron is composed of virtual regular tetrahedrons, the relationships between the coordinates of the vertices and side lengths are unique. Linear scale and squareness errors are measured using an error synthesis model with a least-squares approach. The method was applied to a real machine tool, and performance was verified by confirming that the maximum L^2 norm of volumetric error is improved from 57.6 to 32.8 μm after compensating for the measured geometric errors. Thus, the validity of the proposed method was confirmed by an improvement of 43% in volumetric error. The measurement results were confirmed by the circular tests of ISO 230-4; the peak-to-valley radial deviation improved from 16.0 to 11.2 μm after compensation, and the proposed method contributed to a 30% improvement in the radial deviation.

Keywords Geometric error · Interim check · Machine tools · Virtual polyhedron · Volumetric error

List of Symbols

m	Number of vertices of the virtual polyhedron
c_i	Linear scale error of the linear axis i ($i = X, Y, Z$) (μm/mm)
s_{ij}	Squareness error of linear axis j around axis i ($i, j = X, Y, Z$) (rad)
L	Nominal side length of the virtual polyhedron (mm)
$\delta L_{i,j}$	Measured deviations of the side lengths between the i-th and j-th vertices of the virtual polyhedron ($i, j = 1, \ldots, m$) (mm)
$\boldsymbol{P}_{i,n}\ (x_{i,n}, y_{i,n}, z_{i,n})$	Nominal coordinates of the i-th vertex of the virtual polyhedron ($i = 1, \ldots, m$) (mm)
$\boldsymbol{P}_{i,c}\ (x_{i,c}, y_{i,c}, z_{i,c})$	Coordinates of the i-th vertex of the virtual polyhedron in **{P}** ($i = 1, \ldots, m$) (mm)
$\boldsymbol{P}_{i,a}\ (x_{i,a}, y_{i,a}, z_{i,a})$	Coordinates of the i-th vertex of the virtual polyhedron in **{R}** ($i = 1, \ldots, m$) (mm)
$\delta P_{i,c}\ (\delta x_{i,c}, \delta y_{i,c}, \delta z_{i,c})$	Positional errors between $\boldsymbol{P}_{i,c}$ and $\boldsymbol{P}_{i,n}$ ($i = 1, \ldots, m$) (mm)
$\delta P_{i,a}\ (\delta x_{i,a}, \delta y_{i,a}, \delta z_{i,a})$	Volumetric errors at the i-th vertex ($i = 1, \ldots, m$) (mm)
$\{\boldsymbol{i}\}$	Coordinate system of axis i, ($i = X, Y, Z$)

✉ Seung-Han Yang
syang@knu.ac.kr

Kwang-Il Lee
kilee@kiu.kr

Heung-Ki Jeon
mailgmdrl523@knu.ac.kr

Jae-Chang Lee
jclee@ync.ac.kr

[1] School of Mechanical and Automotive Engineering, Kyungil University, 50, Gamasil-gil, Hayang-eup, Gyeongsan-si, Gyeongbuk 38428, Republic of Korea

[2] School of Mechanical Engineering, Kyungpook National University, 80, Daehak-ro, Buk-gu, Daegu 41566, Republic of Korea

[3] Division of Mechanical Engineering Technology, Yeungnam University College, 170, Hyeonchung-ro, Nam-gu, Daegu 42415, Republic of Korea

$\{P\}$, $\{R\}$	Virtual polyhedron and reference coordinate systems, respectively
$\boldsymbol{\tau}_i^j$	4×4 homogeneous transformation matrix from the j to i coordinate system

1 Introduction

The volumetric errors of machine tools are positional deviations between the nominal and actual positions of the tool in the workpiece coordinate system [1]; they are caused by geometric, thermally induced, and dynamic errors [2]. It is essential to measure geometric errors; together with thermally induced errors, they constitute 60–70% of all volumetric errors and are direct measurements of other errors [3]. The volumetric errors of three-axis machine tools are modeled using 23 geometric errors, including 6 position-dependent geometric errors (PDGEs) for each axis, 3 position-independent geometric errors (PIGEs) between linear axes, and 2 PIGEs of the spindle axis [4–6].

Geometric errors are measured using both direct and indirect methods [7, 8]. Each single axis is controlled when measuring its errors. More than one axis is controlled when inferring geometric errors from measured data. For linear axes, a laser interferometer is widely used to measure geometric errors either separately [9] or simultaneously [10]. For five-axis machine tools, geometric errors of the linear axes are measured by regulating the illumination direction of a laser interferometer through rotary axis control [11]. In addition, a hybrid method featuring a laser interferometer and double ball-bar (DBB) has been developed to measure squareness errors between linear axes over the entire motion of the axes [12]. Using a theory based on a global positioning system, multilateration methods have been developed to measure all geometric errors [13, 14]. DBB methods are also widely used to measure geometric errors via simple circular tests [15, 16]. The DBB test can be generalized by reference to the kinematic structure of the machine tool [17]. In the artefact methods, a straight edge and five capacitive sensors optimally measure geometric errors simultaneously [18]. A ball plate with a three-dimensional probe is used to directly measure volumetric errors; the geometric errors are then inferred via error modeling [19]. Geometric errors can also be measured using an uncalibrated master balls artefact enriched with a ball bar artefact [20]. For the spindle axis, a test mandrel and dial gauge are used to detect parallelism errors by measuring radial deviations in two directions [21]. In addition, DBB circular tests using tools of different lengths can reveal parallelism errors of the spindle axis [22].

However, these approaches require expensive devices, complex measuring processes, long measuring times, and skillful operators; it is expensive to measure all 23 geometric errors. It is thus reasonable to measure only the principal geometric errors when aiming to improve volumetric errors. Circular tests using a DBB are widely applied to measure the principal geometric errors [23]. However, circular tests require simultaneous control of two or more axes; thus, because the measurement results are affected by the dynamic errors of the axes, they do not accurately measure the principal geometric errors of the workspace. A method based on a virtual regular tetrahedron and DBB has been used to measure the principal geometric errors [24, 25]. However, the results are valid only within the volume of the tested regular tetrahedron. Therefore, we devised a method to periodically check the volumetric errors (and thus measure the principal geometric errors) in the workspace of a machine tool, to ensure machining accuracy.

Our method allows cost-effective interim checking of the volumetric and principal geometric errors of machine tools. Section 2 introduces the method, which uses a virtual polyhedron and DBB, and the algorithm for volumetric and geometric error analysis. We verified the method using a machine tool without and with compensation of the measured geometric errors, and also by performing the circular tests of ISO 230-4 (Sect. 3). The main findings and conclusions are summarized in Sect. 4.

2 Measurement of Volumetric and Geometric Errors

The principal geometric errors are linear scale errors for each linear axis, and squareness errors between linear axes, as shown in Fig. 1.

The virtual polyhedron consists of multiple regular tetrahedrons covering the workspace of the machine tool; there are m vertices and the nominal side length is L (Fig. 2). This ensures that the relationships between the coordinates of the vertices and side lengths are unique due to the regular tetrahedrons [26]. Thus, volumetric errors at the vertices can be quantified using the coordinates of the vertices calculated using the measured side lengths. In addition, the nominal side length of the polyhedron is given as L; thus, a DBB accurately measures the side length $L+\delta L_{i,j}$ as the tool is sequentially moved to neighboring vertices. For the experiments in Sect. 3, we used a virtual polyhedron with 24 vertices, 69 sides, and a nominal side length $L=150$ mm. The measurement procedure is summarized in Fig. 3.

We define a coordinate system $\{\boldsymbol{P}\}$ used to calculate the coordinates $\boldsymbol{P}_{i,c}$ ($i=1, \ldots, m$) of the vertices using the measured side lengths $L+\delta L_{i,j}$. Thus, vertices $\boldsymbol{P}_{i,c}$ ($i=1, 2, 3$) are used to define the origin, Y-axis, and YZ-plane, respectively, of the coordinate system $\{\mathbf{P}\}$. The positional errors $\delta P_{i,c}$ ($i=1, 2, 3$) are then given by Eq. (1):

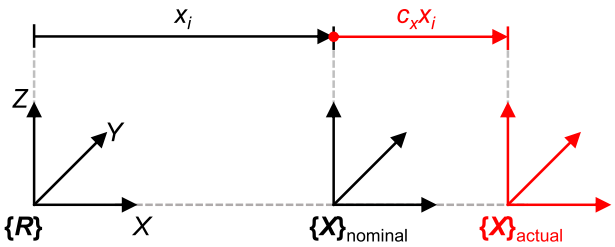

(a) Linear scale error of X-axis.

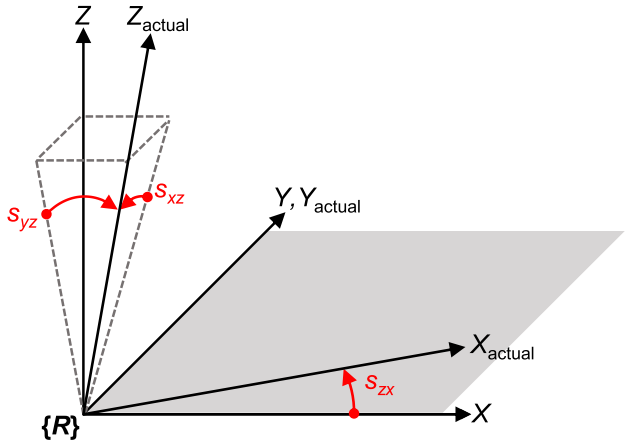

(b) Squareness errors between linear axes.

Fig. 1 Principal geometric errors of three-axis machine tools

$$\begin{aligned} \delta P_{1,c} &= (0,0,0), \\ \delta P_{2,c} &= (0,\delta y_2,0), \\ \delta P_{3,c} &= (0,\delta y_3,\delta z_3) \end{aligned} \tag{1}$$

The relationships between the measured side lengths $L+\delta L_{i,j}$ and two neighboring vertices $\boldsymbol{P}_{i,c}$, $\boldsymbol{P}_{j,c}$ are given by Eq. (2) and linearized using Eq. (3) under small value assumptions:

$$\left\|\mathbf{P}_{i,c}-\mathbf{P}_{j,c}\right\|^2 = \left(L+\delta L_{i,j}\right)^2 \tag{2}$$

$$(x_i-x_j)(\delta x_i-\delta x_j)+(y_i-y_j)(\delta y_i-\delta y_j)+(z_i-z_j)(\delta z_i-\delta z_j)=L\cdot\delta L_{i,j} \tag{3}$$

The relationship between vertex coordinate $\boldsymbol{P}_{i,c}$ and measured side length $L+\delta L_{i,j}$ is unique because the virtual polyhedron consists of multiple regular polyhedrons (as mentioned above). However, several vertices are over-constrained, as shown in Fig. 2 (in blue). Thus, the virtual polyhedron used in Sect. 3 has 66 unknown components of positional errors $\delta P_{i,c}$; however, the number of measured side lengths is 69 (attributable to the over-constraint). Therefore, the unknown components of the positional errors $\delta P_{i,c}$ are calculated using a least-squares method, and the general relationships between these components and the measured side lengths $L+\delta L_{i,j}$ are as given by Eq. (4).

$$\mathbf{Ax}=\mathbf{b} \tag{4}$$

where,

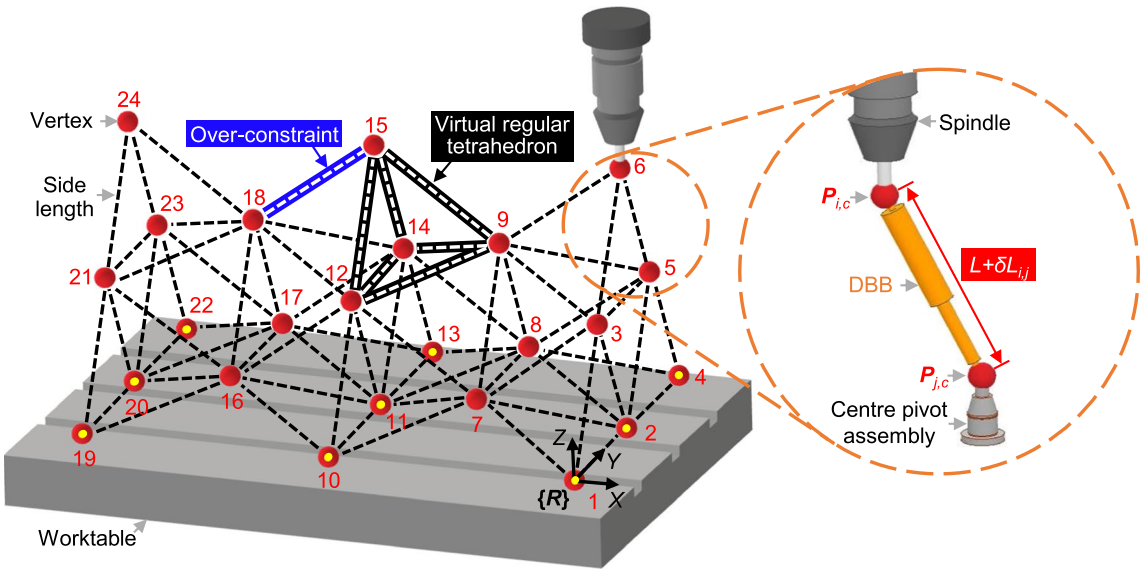

Fig. 2 Virtual polyhedron on the machine tool worktable

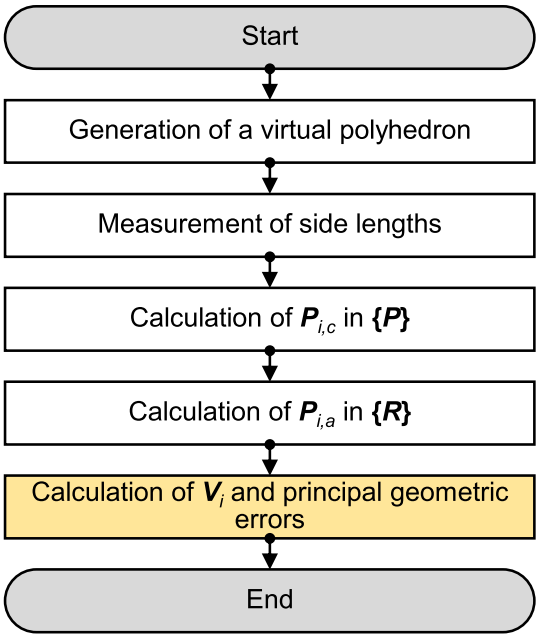

Fig. 3 Measurement procedures of the volumetric and principal geometric errors

plane derived using vertices $\boldsymbol{P}_{i,c}$ with nominal coordinates $z_{i,n}=0$ (the red points with yellow centers in Fig. 2). Vertices $\boldsymbol{P}_{i,a}$ are calculated by transforming vertices $\boldsymbol{P}_{i,c}$ into the coordinate system {**R**}. Finally, the volumetric errors $\delta P_{i,a}$ are calculated as the actual coordinates $\boldsymbol{P}_{i,a}$ minus the nominal coordinates $\boldsymbol{P}_{i,n}$. To derive the principal geometric errors from the calculated volumetric errors $\delta P_{i,a}$, we constructed an error synthesis model for the experimental machine tool described in Sect. 3. This model is given by Eq. (5); it is based on the homogeneous transformation matrix method [27].

$$\boldsymbol{\tau}_W^t = \begin{bmatrix} x_{i,a} & y_{i,a} & z_{i,a} & 1 \end{bmatrix}^T = (\boldsymbol{\tau}_R^Y \boldsymbol{\tau}_Y^X \boldsymbol{\tau}_X^W)^{-1} \boldsymbol{\tau}_R^Z \boldsymbol{\tau}_Z^t \tag{5}$$

where,

$$\boldsymbol{\tau}_R^Y = \begin{bmatrix} 1 & 0 & 0 & 0 \\ 0 & 1 & 0 & -y_{i,n} + c_y y_{i,n} \\ 0 & 0 & 1 & 0 \\ 0 & 0 & 0 & 1 \end{bmatrix},$$

$$\boldsymbol{\tau}_Y^X = \begin{bmatrix} 1 & -s_{zx} & 0 & -x_{i,n} + c_x x_{i,n} \\ s_{zx} & 1 & 0 & -s_{zx} x_{i,n} \\ 0 & 0 & 1 & 0 \\ 0 & 0 & 0 & 1 \end{bmatrix},$$

$$\mathbf{A} = \left[\begin{array}{cccccccc|cccccccc|cccccccc} x_{1,2} & -x_{1,2} & 0 & 0 & \cdots & 0 & 0 & 0 & y_{1,2} & -y_{1,2} & 0 & 0 & \cdots & 0 & 0 & 0 & z_{1,2} & -z_{1,2} & 0 & 0 & \cdots & 0 & 0 & 0 \\ x_{1,3} & 0 & -x_{1,3} & 0 & \cdots & 0 & 0 & 0 & y_{1,3} & 0 & -y_{1,3} & 0 & \cdots & 0 & 0 & 0 & z_{1,3} & 0 & -z_{1,3} & 0 & \cdots & 0 & 0 & 0 \\ \vdots & \vdots & \vdots & \vdots & \ddots & \vdots & \vdots & \vdots & \vdots & \vdots & \vdots & \vdots & \ddots & \vdots & \vdots & \vdots & \vdots & \vdots & \vdots & \vdots & \ddots & \vdots & \vdots & \vdots \\ 0 & x_{2,3} & -x_{2,3} & 0 & \cdots & 0 & 0 & 0 & 0 & y_{2,3} & -y_{2,3} & 0 & \cdots & 0 & 0 & 0 & 0 & z_{2,3} & -z_{2,3} & 0 & \cdots & 0 & 0 & 00 \\ 0 & x_{2,4} & 0 & -x_{2,4} & \cdots & 0 & 0 & 0 & 0 & y_{2,4} & 0 & -y_{2,4} & \cdots & 0 & 0 & 0 & 0 & z_{2,4} & 0 & -z_{2,4} & \cdots & 0 & 0 & 0 \\ \vdots & \vdots & \vdots & \vdots & \ddots & \vdots & \vdots & \vdots & \vdots & \vdots & \vdots & \vdots & \ddots & \vdots & \vdots & \vdots & \vdots & \vdots & \vdots & \vdots & \ddots & \vdots & \vdots & \vdots \\ 0 & 0 & 0 & 0 & \cdots & x_{22,23} & -x_{22,23} & 0 & 0 & 0 & 0 & 0 & \cdots & y_{22,23} & -y_{22,23} & 0 & 0 & 0 & 0 & 0 & \cdots & z_{22,23} & -z_{22,23} & 0 \\ 0 & 0 & 0 & 0 & \cdots & 0 & x_{23,24} & -x_{23,24} & 0 & 0 & 0 & 0 & \cdots & 0 & y_{23,24} & -y_{23,24} & 0 & 0 & 0 & 0 & \cdots & 0 & z_{23,24} & -z_{23,24} \end{array}\right],$$

$$\mathbf{x} = \begin{bmatrix} \delta x_1 & \cdots & \delta x_{24} & \delta y_1 & \cdots & \delta y_{24} & \delta z_1 & \cdots & \delta z_{24} \end{bmatrix}^T,$$

$$\mathbf{b} = L \cdot \begin{bmatrix} \delta L_{1,2} & \cdots & \delta L_{1,24} & \delta L_{2,3} & \cdots & \delta L_{2,24} & \cdots & \delta L_{22,23} & \delta L_{22,24} & \delta L_{23,24} \end{bmatrix}^T,$$

$$k_{i,j} = k_i - k_j \quad (k = x, y, z)$$

Note that coordinate system {**P**}, established using only vertices $\boldsymbol{P}_{i,c}$ ($i=1, 2, 3$) of the virtual polyhedron, is not the same as coordinate system {**R**} of the experimental machine tool. However, the origins of coordinate systems {**P**} and {**R**} are the same: $\boldsymbol{P}_{1,c}=\boldsymbol{P}_{1,a}$. Thus, vertices $\boldsymbol{P}_{i,c}$ ($i=1, 2, 4$) are used to define the least-squares reference straight line of the Y-axis [4]. The YZ-plane for coordinate system {**R**} is the least-squares

$$\boldsymbol{\tau}_X^W = \begin{bmatrix} 1 & 0 & 0 & 0 \\ 0 & 1 & 0 & 0 \\ 0 & 0 & 1 & 0 \\ 0 & 0 & 0 & 1 \end{bmatrix},$$

$$\boldsymbol{\tau}_R^Z = \begin{bmatrix} 1 & 0 & s_{yz} & s_{yz} z_{i,n} \\ 0 & 1 & -s_{xz} & -s_{xz} z_{i,n} \\ -s_{yz} & s_{xz} & 1 & z_{i,n} + c_z z_{i,n} \\ 0 & 0 & 0 & 1 \end{bmatrix},$$

$$\boldsymbol{\tau}_Z^t = \begin{bmatrix} 0 \\ 0 \\ 0 \\ 1 \end{bmatrix}$$

Therefore, the relationships between the volumetric errors $\delta P_{i,a}$ and principal geometric errors are determined as shown in Eq. (6), and the errors are calculated by applying a least-squares method.

$$\begin{bmatrix} \delta x_{1,a} \\ \delta y_{1,a} \\ \delta z_{1,a} \\ \vdots \\ \delta x_{24,a} \\ \delta y_{24,a} \\ \delta z_{24,a} \end{bmatrix} = \begin{bmatrix} -x_{1,n} & 0 & 0 & y_{1,n} & 0 & z_{1,n} \\ 0 & -y_{1,n} & 0 & 0 & -z_{1,n} & 0 \\ 0 & 0 & z_{1,n} & 0 & 0 & 0 \\ \vdots & \vdots & \vdots & \vdots & \vdots & \vdots \\ -x_{24,n} & 0 & 0 & y_{24,n} & 0 & z_{24,n} \\ 0 & -y_{24,n} & 0 & 0 & -z_{24,n} & 0 \\ 0 & 0 & z_{24,n} & 0 & 0 & 0 \end{bmatrix} \begin{bmatrix} c_x \\ c_y \\ c_z \\ s_{zx} \\ s_{xz} \\ s_{yz} \end{bmatrix} \tag{6}$$

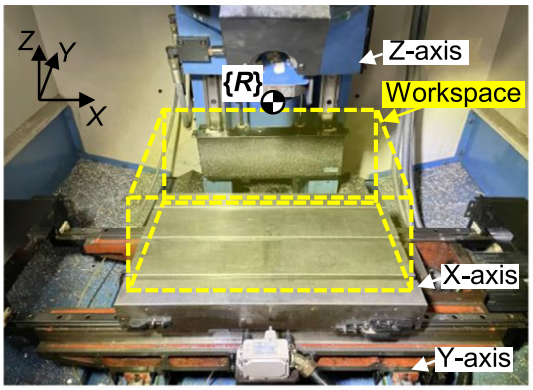

(a) Kinematic structure of the machine tool.

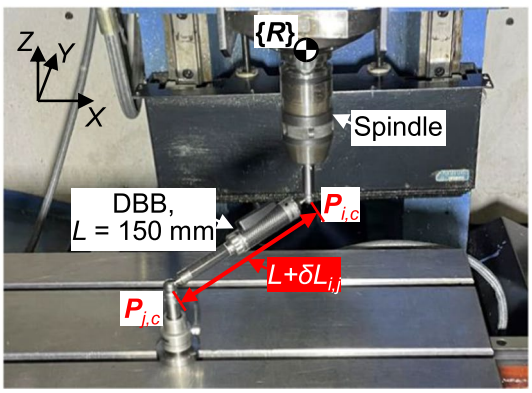

(b) Sequential measurements of side lengths

Fig. 4 Experimental machine tool and DBB set-up

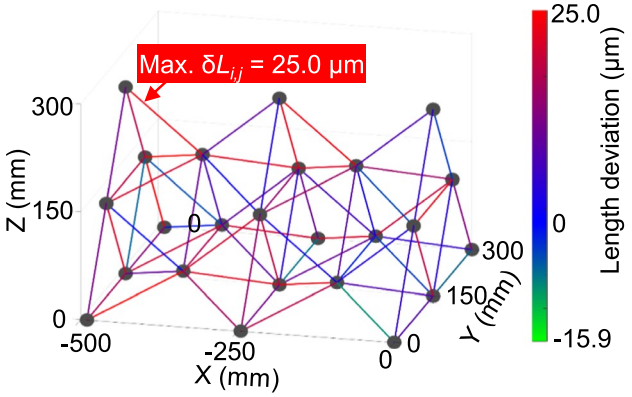

(a) Without compensation.

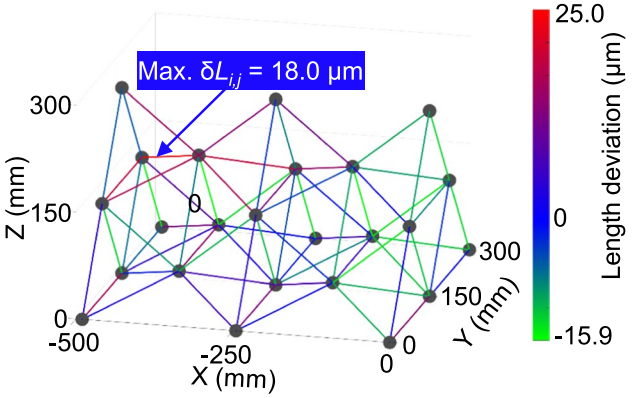

(b) With compensation.

Fig. 5 Measured side lengths of the virtual polyhedron

3 Experimental

3.1 Interim Checks of Volumetric and Principal Geometric Errors

The method described in Sect. 2 was applied to a machine tool (SPT-T30; Komatec Co. Ltd., Republic of Korea) as shown in Fig. 4a, and the side lengths were sequentially measured using a DBB (QC20-W; Renishaw Co. Ltd., UK) as shown in Fig. 4b. It takes 40 min to measure all side lengths shown in Fig. 2.

As mentioned in Sect. 2, the virtual polyhedron has 24 vertices and 69 sides of nominal length $L = 150$ mm. The polyhedron length deviation $\delta L_{i,j}$ is large (maximum = 25.0 μm), attributable mainly to geometric errors (Fig. 5a).

By inserting the measured side length $L + \delta L_{i,j}$ into Eq. (4), the vertices $\boldsymbol{P}_{i,a}$ are calculated as shown in Fig. 6a. They also exhibit large positional deviations (volumetric errors) relative to the nominal vertices $\boldsymbol{P}_{i,n}$. These must be improved by deriving and compensating for the principal

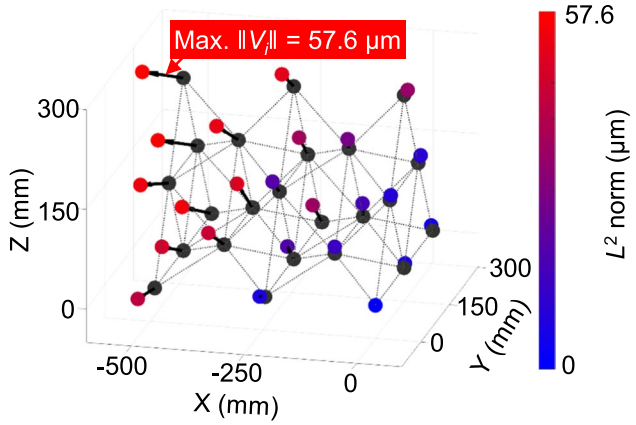

(a) Without compensation.

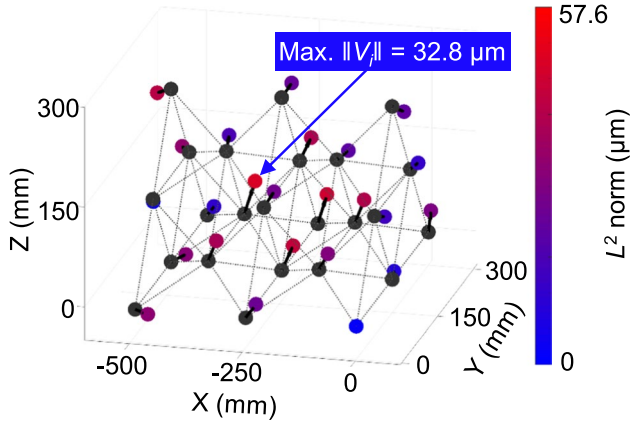

(b) With compensation.

Fig. 6 Vertices calculated using the measured side lengths

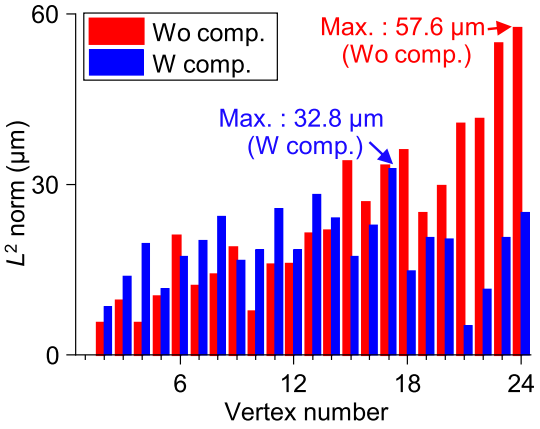

Fig. 8 L^2 norms of volumetric errors without and with compensation

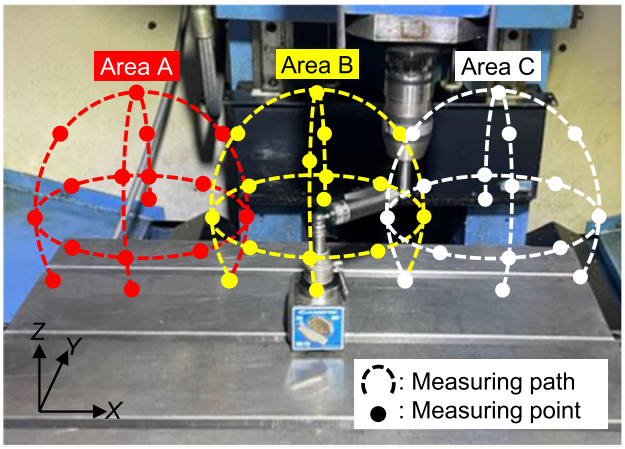

Fig. 9 Static circular paths that cover the workspace of the machine tool

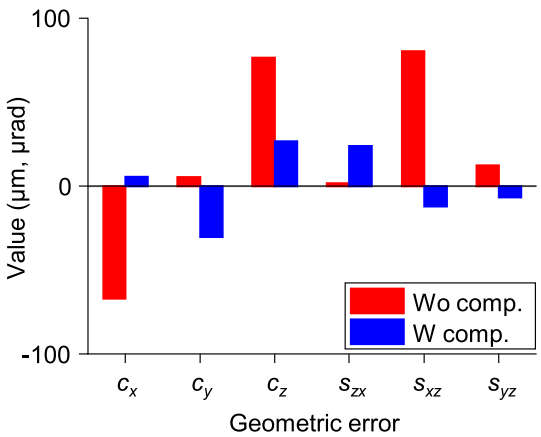

Fig. 7 Principal geometric errors measured without and with compensation

geometric errors. The latter errors are derived by inserting the volumetric errors into Eq. (6) (Fig. 7).

For verification, the virtual polyhedron was re-measured after compensating for the principal measured geometric errors. Here, G-code-based compensation was conducted by additional movement of the linear axes as volumetric errors in Eq. (5). Both the measured side lengths and volumetric errors improved (Figs. 5b and 6b, respectively), as did the principal geometric errors (Fig. 7). The maximum L^2 norms of the volumetric errors were 57.6 and 32.8 μm without and with compensation of the principal geometric errors, respectively (Fig. 8), showing an improvement of approximately 43% for the volumetric error using the proposed method. Here, the maximum L^2 norm is used as a criterion to evaluate volumetric error because it coincides with the worst-case scenario.

Thus, the volumetric errors of the machine tool were improved significantly after compensating for the principal measured geometric errors. However, residual side length,

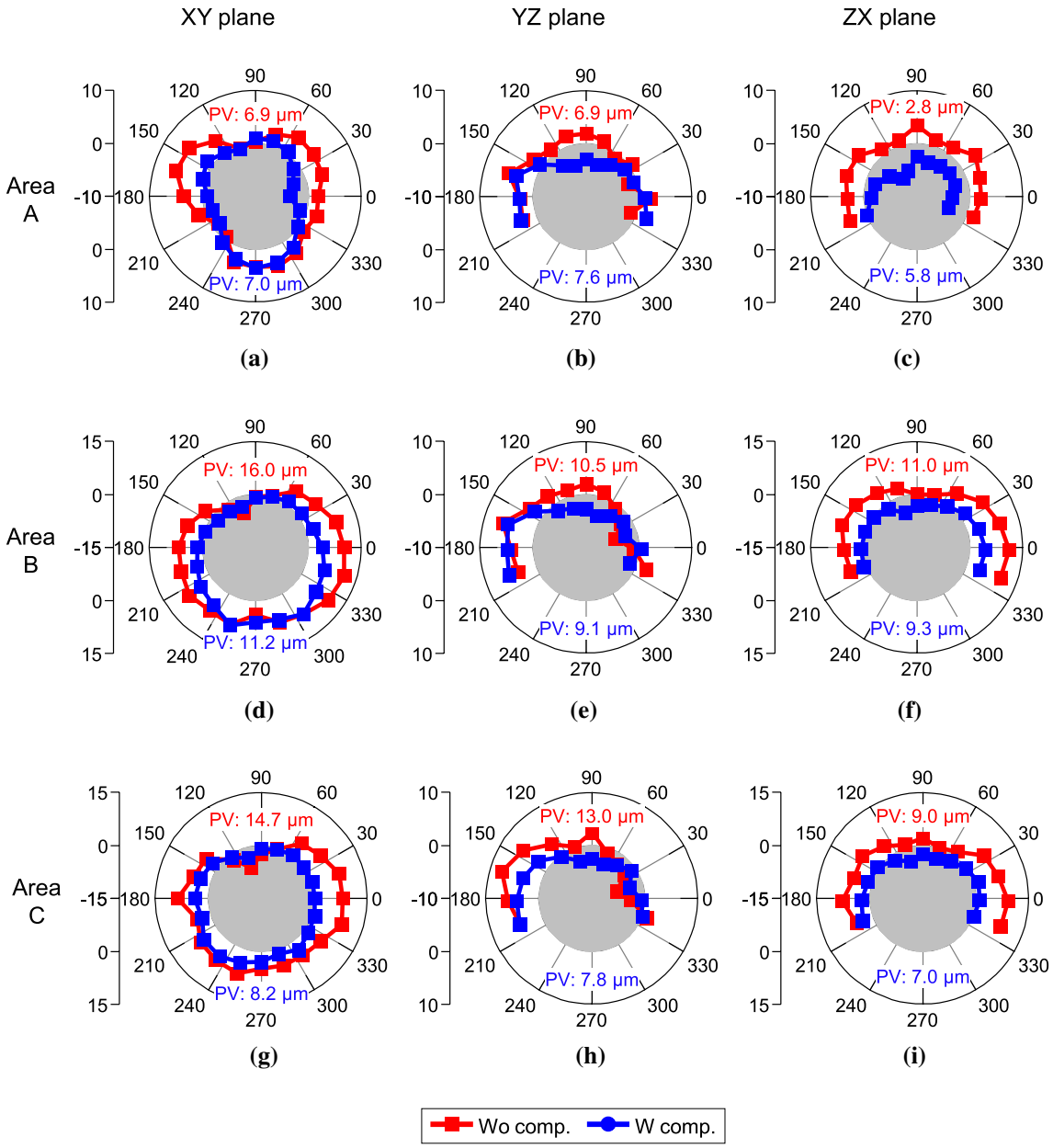

Fig. 10 Measured radial deviations without and with compensation

volumetric and principal geometric errors remain; these may be attributable to other geometric errors. We aimed to improve volumetric errors by measuring and compensating for the principal geometric errors only, instead of all 23 geometric errors.

3.2 Verification Using Static Circular Tests

The principal measured geometric errors shown in Fig. 7 were additionally verified using the static circular tests of ISO 230-4 and the DBB employed above (Fig. 9). These tests check the effects of principal geometric errors only within defined test volumes. The circular paths in the XY, YZ, and ZX planes of the single set-ups established in Areas A–C to cover the workspace of the machine tool. The measuring ranges of the circular paths in the XY, YZ, and ZX planes are [0°, 360°], [− 20°, 200°], and [− 110°, 110°] respectively; the nominal path radius is 100 mm. The measured radial deviations of the circular paths are shown in Fig. 10. The maximum peak-to-valley (PV) values are 16.0 and 11.2 μm without and with compensation, respectively, proving the validity of the measured geometric errors by an improvement of 30% in the radial deviation. Note that the PV values are increased in Area A, but

considerably decreased in Areas B and C, perhaps because the volumetric errors were regulated over the workpiece (by compensating for the principal geometric errors), thus improving the maximum volumetric error.

4 Conclusion

We developed a method for interim checking and improvement of the volumetric errors of machine tools, with the aim of enhancing volumetric accuracy. We used the side lengths of a virtual polyhedron to derive the volumetric and principal geometric errors. Our cost-effective method can be used to rapidly improve volumetric errors for only the principal geometric errors. However, because it compensates only for the principal geometric errors, periodic interim checks are required. Our main findings are as follows.

First, three-dimensional volumetric errors are measurable using the one-dimensional side lengths of a virtual polyhedron consisting of multiple regular tetrahedrons. The volume of the virtual polyhedron is controlled by changing the nominal side length, and via attachment of additional regular tetrahedron over the workspace of a machine tool. Thus, the cost of volumetric error measurement is reduced; only a DBB is required.

Second, it is important to maintain volumetric accuracy by regularly checking for volumetric and principal geometric errors over the machine tool workspace. We measured and compensated for principal geometric errors using a virtual polyhedron containing the workspace volume. This does not yield local improvements. However, it is a practical method to maintain overall volumetric accuracy.

Third, the principal geometric errors can be measured by performing circular tests in the XY, YZ, and ZX planes. However, the measured errors are valid only within the volumes of the circular tests, and not over the workspace as a whole. This is true even if circular tests are performed at different positions within the workspace, because the test results are not interrelated. Thus, circular tests performed at different positions improve volumetric errors only indirectly, by compensating for the principal geometric errors.

Acknowledgements This work was supported by the National Research Foundation of Korea (NRF) grant funded by the Korea government (MSIT) (Nos. 2020R1C1C100330011 and 2019R1A2C2088683).

Funding This work was supported by the National Research Foundation of Korea (NRF) grant funded by the Korea government (MSIT) (Nos. 2020R1C1C100330011 and 2019R1A2C2088683).

Declarations

Competing interests The authors declare that they have no conflict of interest.

References

1. Okafor, A. C., & Ertekin, Y. M. (2000). Derivation of machine tool error models and error compensation procedure for three axes vertical machining center using rigid body kinematics. *International Journal of Machine Tools and Manufacture, 40*, 1199–1213. https://doi.org/10.1016/S0890-6955(99)00105-4
2. Yang, S. H., & Lee, K. I. (2021). Machine tool analyzer: A device for identifying 13 position–independent geometric errors for five–axis machine tools. *The International Journal of Advanced Manufacturing Technology, 115*, 2945–2957. https://doi.org/10.1007/s00170-021-07341-7
3. Ramesh, R., Mannan, M. A., & Poo, A. N. (2000). Error compensation in machine tools—A review Part I: Geometric, cutting–force induced and fixture–dependent errors. *International Journal of Machine Tools and Manufacture, 40*, 1235–1256. https://doi.org/10.1016/S0890-6955(00)00009-2
4. ISO 230-1. (2012). Test code for machine tools—Part 1: Geometric accuracy of machines operating under no-load or quasi-static conditions. *ISO*.
5. Lee, J. C., Lee, H. H., & Yang, S. H. (2016). Total measurement of geometric errors of a three–axis machine tool by developing a hybrid technique. *International Journal of Precision Engineering and Manufacturing, 17*, 427–432. https://doi.org/10.1007/s12541-016-0053-5
6. ISO 230–7. (2015). Test code for machine tools—Part 7: Geometric accuracy of axes of rotation. *ISO*.
7. Schwenke, H., Knapp, W., Haitjema, H., Weckenmann, A., Schmitt, R., & Delbressine, F. (2008). Geometric error measurement and compensation of machines – An update. *CIRP Annals Manufacturing Technology, 57*, 660–675. https://doi.org/10.1016/j.cirp.2008.09.008
8. Ibaraki, S., & Knapp, W. (2012). Indirect measurement of volumetric accuracy for three–axis and five–axis machine tools: A review. *International Journal of Automation Technology, 6*, 110–124. https://doi.org/10.20965/ijat.2012.p0110
9. ISO 230–2. (2014). Test code for machine tools—Part 2: Determination of accuracy and repeatability of positioning of numerically controlled axes. *ISO*.
10. Sun, G., He, G., Zhang, D., Yao, C., & Tian, W. (2020). Body diagonal error measurement and evaluation of a multiaxis machine tool using a multibeam laser interferometer. *The International Journal of Advanced Manufacturing Technology, 107*, 4545–4559. https://doi.org/10.1007/s00170-020-05275-0
11. Ibaraki, S., & Hiruya, M. (2021). A novel scheme to measure 2D error motions of linear axes by regulating the direction of a laser interferometer. *Precision Engineering, 67*, 152–159. https://doi.org/10.1016/j.precisioneng.2020.09.011
12. Lee, H. H., Lee, D. M., & Yang, S. H. (2014). A technique for accuracy improvement of squareness estimation using a double ball–bar. *Measurement Science and Technology, 25*, 094009. https://doi.org/10.1088/0957-0233/25/9/094009

13. Schwenke, H., Schmitt, R., Jatzkowski, P., & Warmann, C. (2009). On–the–fly calibration of linear and rotary axes of machine tools and CMMs using a tracking interferometer. *CIRP Annals, 58*, 477–480. https://doi.org/10.1016/j.cirp.2009.03.007
14. Zha, J., Wang, T., Li, L., & Chen, Y. (2020). Volumetric error compensation of machine tool using laser tracer and machining verification. *The International Journal of Advanced Manufacturing Technology, 7–8*, 2467–2481. https://doi.org/10.1007/s00170-020-05556-8
15. ISO 230–4. (2005). Test code for machine tools—Part 4: Circular tests for numerically controlled machine tools. *ISO*.
16. Pahk, H. J., Kim, Y. S., & Moon, J. H. (1994). A new technique for volumetric error assessment of CNC machine tools incorporating ball bar measurement and 3D volumetric error model. *International Journal of Machine Tools and Manufacture, 37*, 1583–1596. https://doi.org/10.1016/S0890-6955(97)00029-1
17. Wang, Z., Wang, D., Yu, S., Li, X., & Dong, H. (2021). A reconfigurable mechanism model for error identification in the double ball bar test of machine tools. *International Journal of Machine Tools and Manufacture, 165*, 103737. https://doi.org/10.1016/j.ijmachtools.2021.103737
18. Lee, K. I., Lee, J. C., & Yang, S. H. (2013). The optimal design of a measurement system to measure the geometric errors of linear axes. *The International Journal of Advanced Manufacturing Technology, 66*, 141–149. https://doi.org/10.1007/s00170-012-4312-z
19. Liebrich, T., Bringmann, B., & Knapp, W. (2009). Calibration of a 3D–ball plate. *Precision Engineering, 33*, 1–6. https://doi.org/10.1016/j.precisioneng.2008.02.003
20. Mayer, J. R. R. (2012). Five–axis machine tool calibration by probing a scale enriched reconfigurable uncalibrated master balls artefact. *CIRP Annals – Manufacturing Technology, 61*, 515–518. https://doi.org/10.1016/j.cirp.2012.03.022
21. ISO 10791–2. (2001). Test conditions for machining centres Part 2: Geometric tests for machines with vertical spindle or universal heads with vertical primary rotary axis. *ISO*.
22. Lee, K. I., Shin, D. H., & Yang, S. H. (2017). Parallelism error measurement for the spindle axis of machine tools by two circular tests with different tool lengths. *The International Journal of Advanced Manufacturing Technology, 88*, 2883–2887. https://doi.org/10.1007/s00170-016-8999-0
23. Yang, S. H., Kim, K. H., Park, Y. K., & Lee, S. G. (2004). Error analysis and compensation for the volumetric errors of a vertical machining centre using a hemispherical helix ball bar test. *The International Journal of Advanced Manufacturing Technology, 23*, 495–500. https://doi.org/10.1007/s00170-003-1662-6
24. Lee, K. I., Lee, H. H., & Yang, S. H. (2017). Interim check and practical accuracy improvement for machine tools with sequential measurements using a double ball–bar on a virtual regular tetrahedron. *The International Journal of Advanced Manufacturing Technology, 93*, 1527–1536. https://doi.org/10.1007/s00170-017-0582-9
25. Yang, S. H., Lee, H. H., & Lee, K. I. (2017). Interim check and compensation of geometric errors to improve volumetric error of machine tools. *Journal of Korean Society for Precision Engineering, 35*, 623–627. https://doi.org/10.7736/KSPE.2018.35.6.623
26. Ziegert, J. C., & Mize, C. D. (1994). The laser ball bar: A new instrument for machine tool metrology. *Precision Engineering, 16*, 259–267. https://doi.org/10.1016/0141-6359(94)90002-7
27. Lee, D. M., & Yang, S. H. (2010). Mathematical approach and general formulation for error synthesis modeling of multi–axis system. *International Journal of Modern Physics B, 24*, 2737–2742. https://doi.org/10.1142/S0217979210065556

Kwang-Il Lee received the Ph.D. degree in mechanical engineering from the Kyungpook National University, Daegu, Republic of Korea. He is currently a professor in the School of Mechanical and Automotive Engineering, Kyungil University. His research interest is precision methodologies for machine tools, precision robots, and 3D printers.

Heung-Ki Jeon is a M.Sc. Candidate in the Department of Mechanical Engineering, Kyungpook National University, Daegu, Republic of Korea. His research interest is machine tool calibrations.

Jae-Chang Lee received the Ph.D. degree in mechanical engineering from the Kyungpook National University, Daegu, Republic of Korea. He is currently a professor in the Division of Mechanical Engineering Technology, Yeungnam University College. His research interest is designs and controls for ultra-precision machine tools.

Seung-Han Yang received the Ph.D. degree in mechanical engineering from the University of Michigan, Ann Arbor, Michigan, USA. He is currently a professor in the School of Mechanical Engineering, Kyungpook National University. His research interest is intelligent manufacturing systems and CAD/CAM.